Technical Report CERC-89-9
August 1998

US Army Corps of Engineers
Waterways Experiment Station

Coastal Engineering Research Program

SBEACH: Numerical Model for Simulating Storm-Induced Beach Change

Report 5
Representation of Nonerodible (Hard) Bottoms

by Magnus Larson, University of Lund
Nicholas C. Kraus, WES

Prepared for Headquarters, U.S. Army Corps of Engineers

The contents of this report are not to be used for advertising, publication, or promotional purposes. Citation of trade names does not constitute an official endorsement or approval of the use of such commercial products.

The findings of this report are not to be construed as an official Department of the Army position, unless so designated by other authorized documents.

Coastal Engineering Research Program

Technical Report CERC-89-9
August 1998

SBEACH: Numerical Model for Simulating Storm-Induced Beach Change

Report 5
Representation of Nonerodible (Hard) Bottoms

by Magnus Larson

Department of Water Resources Engineering
Lund University of Technology
University of Lund
Box 118, Lund, Sweden S-221 00

Nicholas C. Kraus

U.S. Army Corps of Engineers
Waterways Experiment Station
3909 Halls Ferry Road
Vicksburg, MS 39180-6199

Report 5 of a series

Approved for public release; distribution is unlimited

Prepared for U.S. Army Corps of Engineers
Washington, DC 20314-1000

Under Work Unit 32530

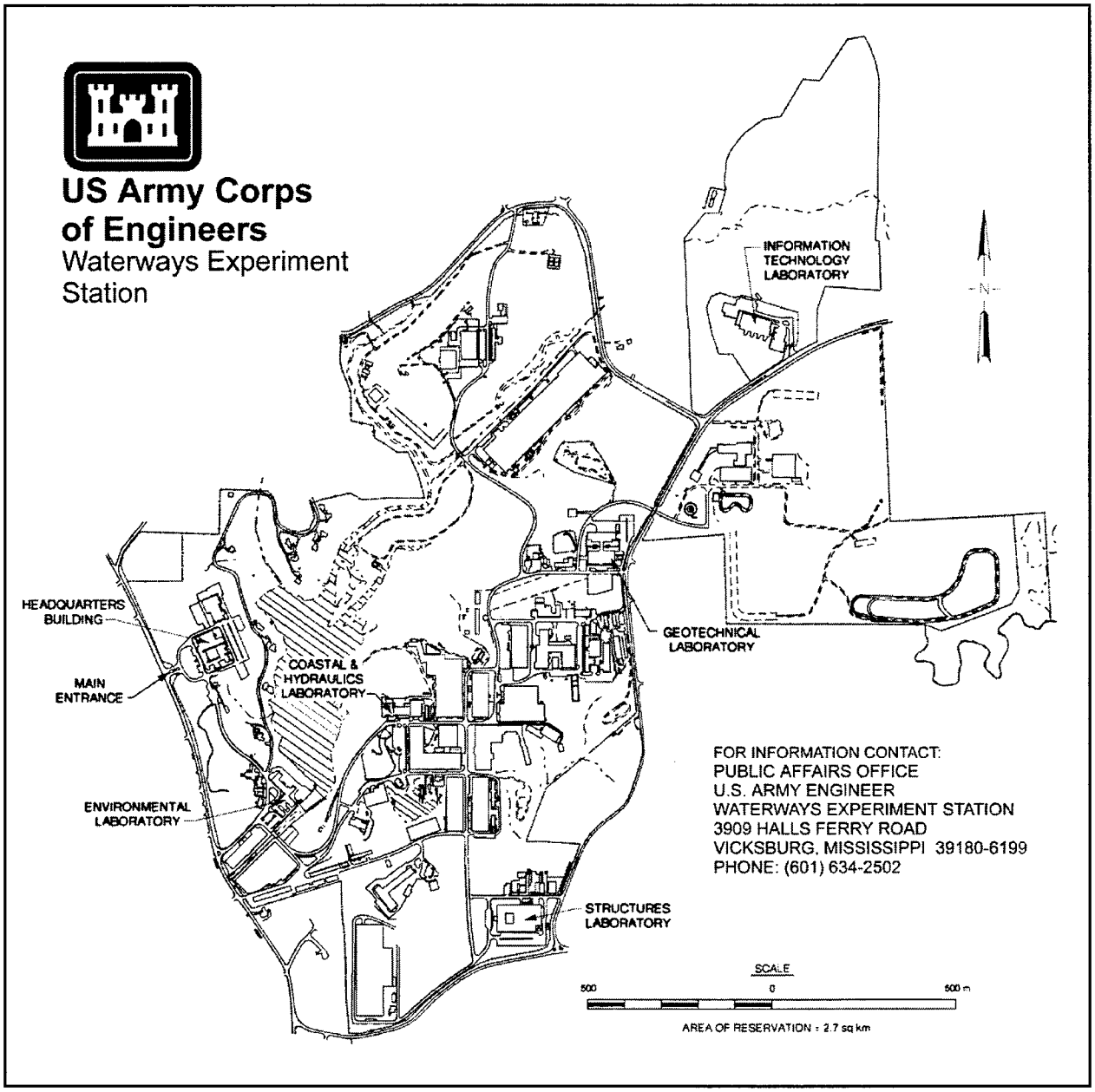

Waterways Experiment Station Cataloging-in-Publication Data

Larson, Magnus.

SBEACH : numerical model for simulating storm-induced beach change. Report 5, Representation of nonerodible (hard) bottoms / by Magnus Larson, Nicholas C. Kraus ; prepared for U.S. Army Corps of Engineers.

44 p. : ill. ; 28 cm. — (Technical report ; CERC-89-9 rept.5)

Includes bibliographic references.

Report 5 of a series.

1. Beach erosion —Mathematical models. 2. Coast changes — Mathematical models. 3. Banks (Oceanography) — Mathematical models. I. Kraus, Nicholas C. II. United States. Army. Corps of Engineers. III. U.S. Army Engineer Waterways Experiment Station. IV. Coastal and Hydraulics Laboratory (U.S. Army Engineer Waterways Experiment Station) V. Coastal Engineering Research Program (U.S.) VI. Title. VII. Title: Numerical model for simulating storm-induced beach change, report 5, representation of nonerodible (hard) bottoms. VIII. Series: Technical report (U.S. Army Engineer Waterways Experiment Station) ; CERC-89-9 rept. 5.

TA7 W34 no.CERC-89-9 rept.5

Contents

List of Figures

List of Tables

Preface

The work described in this report was commissioned by the U.S. Army Engineer District, Jacksonville, under a contract with Texas A&M University-Corpus Christi (TAMU-CC) and coordinated with the U.S. Army Engineer Waterways Experiment Station (WES), Coastal and Hydraulics Laboratory (CHL), Vicksburg, MS. These activities were conducted in support of the U.S. Army Corps of Engineers (USACE) storm-damage reduction mission and beach-fill design activities. Work at CHL was authorized as part of the Civil Works Research and Development Program by Headquarters, U.S. Army Corps of Engineers (HQUSACE), and was performed under the Nearshore Berm and Long-Term Profile Evolution Work Unit 33046, Coastal Navigation and Storm Damage Reduction Program, CHL. Messrs. John H. Lockhart, Jr., (retired) Barry W. Holliday, and Charles Chesnutt were HQUSACE Technical Monitors. Ms. Carolyn M. Holmes was CHL Coastal Program Manager.

Theoretical work was authorized by the Jacksonville District and the study was performed over the period June 1995 to 29 November 1995. Technical Monitors for this project at the Jacksonville District were Mr. Peter Grace, Engineering Division, Hydrology and Hydraulics Branch – Coastal Design Section, and Mr. Thomas Smith, Planning Division, Plan Formulation Branch – Coastal Section. Theoretical work was performed and a preliminary draft of this report written by Dr. Nicholas C. Kraus, formerly of TAMU-CC and presently in the Coastal Sediments and Engineering Division (CSED), CHL, and Dr. Magnus Larson, Department of Water Resources Engineering, University of Lund, Sweden. Technical review of this report was provided by Peter Grace and, Thomas Smith, Jacksonville District, and Mr. Randall A. Wise, Coastal Processes Branch (CPB), CSED, CHL, who was Principal Investigator of the Nearshore Berm and Long-Term Profile Evolution Work Unit. Mr. Wise assisted in generating figures for the final report. Ms. Holley Messing, Civil Engineering Technician, CPB, CSED, CHL, assisted with preparation of the final document.

Work at CHL was performed under the general supervision of Dr. James R. Houston and Mr. Charles C. Calhoun, Jr., Director and Assistant Director, respectively, and the administrative supervision of Mr. Thomas W. Richardson, Chief, CSED, CHL, and Mr. Bruce A. Ebersole, Chief, CPB, CSED, CHL.

At the time of publication of this report, Director of WES was Dr. Robert W. Whalin. Commander was COL Robin R. Cababa, EN.

The contents of this report are not to be used for advertising, publication, or promotional purposes. Citation of trade names does not constitute an official endorsement or approval of the use of such commercial products.

1 Background of the Study

The SBEACH (Storm-induced BEAch CHange) numerical simulation model was developed at the U.S. Army Engineer Waterways Experiment Station, Coastal and Hydraulics Laboratory (CHL), to calculate beach and dune erosion under storm water levels and wave action (Larson and Kraus 1989; Larson, Kraus, and Byrnes 1990; Rosati et al. 1993; Wise, Smith, and Larson 1996).

Numerous applied as well as fundamental studies have been conducted with SBEACH and published in the engineering and scientific literature. Examples are: Larson and Kraus (1991), who discuss beach-fill design with respect to prediction of beach and dune response to hurricanes and extra-tropical storms; Hansen and Byrnes (1991), who calculate optimal beach fill cross sections for Ocean City, Maryland, with a calibrated model; Kraus and Wise (1993) and Wise and Kraus (1993) who describe model predictions for Ocean City, Maryland, for which an overwash algorithm was incorporated in SBEACH; and Wise, Smith, and Larson (1996), who performed extensive testing of SBEACH for the SUPERTANK physical model data (Kraus and Smith 1994; Kraus, Smith, and Sollitt 1992; Smith and Kraus 1995) and for several good-quality field data sets on dune erosion. SBEACH is under continued development and improvement in support of engineering applications.

Orientation to the Hard-Bottom Problem

In this report, a hard bottom (HB) is considered to be a nonerodible bottom feature that may be located anywhere on the subaerial and subaqueous beach. The present work was performed to allow SBEACH to account for nonerodible (hard) bottoms in computing dune and beach erosion. This enhancement was requested by the U.S. Army Engineer District, Jacksonville, to deal with various forms and types of HB such as those presently being encountered in its projects along the beaches of Martin, Brevard, St. Lucie, and Indian River Counties, located on the Atlantic Ocean coast of Florida. The Jacksonville District encounters nonerodible beach and nearshore bottom features along the coasts of Florida, Puerto Rico, and the Virgin Islands. More generally, HB is encountered in a wide range of environments from the coral reefs in the South Pacific to cohesive shores in the Great Lakes. (Strictly speaking, a cohesive bottom will erode, although more slowly than fine clastic sediments, such as sand.)

HB in Florida may consist of worm rock, limestone, coquina, coral reefs, sedimentary rocks, and artificial structures such as dumped concrete and rubble. HB provides habitat for numerous types of marine life. As such, it is considered

to be a resource that must be identified and protected. Natural processes such as cross-shore and longshore sand movement can cover and uncover HB, and HB is subjected to various stresses such as attack by violent wave action, rubbing and breakage by beach walkers, and damage by boat anchors.

Figure 1 is an aerial photograph showing exposed HB in the clear nearshore water off Martin County Beach Park, at Bathtub Reef, Florida. In idealized form, this HB appears as three linear strips oriented approximately with the trend of the shoreline. It is expected that the narrow sand strips lying between the HB plateaus are only veneers of sand temporarily trapped between them. Qualitative observation indicates that sand moves on and off such HB areas according to wave conditions.

Figure 1. Aerial view of nearshore at Martin County Beach Park at Bathtub Reef showing three bands of hard bottoms

Figures 2 and 3 are ground photographs taken at Walton Rocks Beach, St. Lucie County, Florida. The HB shown is built by "honeycomb" (sabellariid) worms (*phragmatopoma caudata*) that gather sand particles and shell fragments and bind them with protein-based secretions.

Figures 4 and 5 show the worm rock at Bathtub Reef, Martin County Beach Park, Florida. In addition to HB exposed on the foreshore at this beach, a substantial outcrop exists on shore that developed during a geologic period of

Figure 2. Ground view of hard bottom (worm rock) at Walton Rocks Beach

Figure 3. Closeup of worm rock at Walton Rocks Beach

Figure 4. Ground view of worm rock on foreshore and upper beach at Bathtub Reef

Figure 5. Massive relic worm rock on upper beach at Bathtub Reef

higher standing water. Such massive outcrops would function as a seawall in protecting the shore and not allowing upland to erode.

Hard-Bottom Calculation Capability

There are several reasons for interest in calculation of dune and beach response to a storm in the presence of HB. First, and most obvious, is the fact that HB on the beach will restrict sand movement because the area occupied by the HB does not contribute to the sediment budget. Calculations performed as if the HB were not there could suggest erosion of the beach faces and dunes that cannot, in fact, erode. Such calculations might also suggest an unrealistic supply of sand to the offshore (that might cover other HB). Another reason is that designers need to know if HB will be covered by cross-shore movement of sand. If HB is predicted to be covered by eroded sand or by a beach fill, mitigation measures might be taken or an alternative design considered. The algorithm developed here is applicable to HB appearing on the dune, foreshore, and surf zone, but not in the far offshore, beyond the influence of breaking waves. This capability is compatible with the basic approach and structure of SBEACH, as described in the next section.

Capabilities and Limitations

SBEACH is an empirically based model that calculates the net cross-shore sand transport rate in four zones from the dune or beach face, through the surf zone, and into the offshore past the deepest break-point bar produced by short-period incident waves (Larson and Kraus 1989). Calculations can be performed for an arbitrary initial beach profile shape and a specified grain size in the sand range, and the inputs may include time series of: water level; wave height, period, and direction; and wind speed and direction. Either monochromatic waves or waves that vary randomly in height can be specified. The wave model is relatively sophisticated and computes wave shoaling, refraction, breaking, breaking wave re-formation, wave- and wind-induced setup and setdown, and runup. SBEACH can generate, grow, move, and deflate the predominant longshore (wave break-point) bar.

SBEACH is applicable primarily to the dune, beach face, and surf zone (including the area of longshore bar). It was not developed to predict details of sediment movement or sediment movement under the (nonbreaking) waves in the offshore. The basic limitations of SBEACH carry over to the HB capability.

Scope of Report

Chapter 1 gives the background and motivation of this study, including capabilities and limitations of the work. Chapter 2 presents the logic behind the HB constraint, together with the mathematical and numerical expressions of the action of HB in SBEACH. Results of several tests of the HB algorithm are described in Chapter 3.

2 Hard-Bottom Algorithm

This chapter presents a formulation of a mathematical description of cross-shore transport over HB. The most obvious function of a nonerodible (hard) bottom is to prevent a lowering of the profile in locations where the HB is exposed. Buried HB does not alter the sand transport and profile evolution, until it becomes exposed. In this respect, HB functions comparably for profile evolution as does a seawall on the shoreline response produced by gradients in longshore transport. Thus, the algorithm presented here to take into account the effect of exposed HB on profile response has many similarities to an algorithm presented by Hanson and Kraus (1985, 1987) for representing seawalls in shoreline change models. Nairn and Riddell (1992) and Nairn and Southgate (1993) presented simulation results obtained with a profile response model that involved cases where a nonerodible bottom was exposed. Although their results appear reasonable, no details were given on the algorithm employed, and it is therefore difficult to assess the generality of the approach, such as, for example, whether the algorithm functions if the transport direction changes direction at arbitrary locations along the profile.

The HB algorithm developed in this study accommodates complex net cross-shore transport rate distributions having several onshore and offshore peaks, as well as any number of HB areas located arbitrarily across the profile. At present, SBEACH typically produces transport rate distributions with the transport directed either onshore or offshore across the entire profile during a particular time-step. However, it is expected that in future versions, additional transport mechanisms will be added that may produce more complex distributions. It was considered advantageous to develop a general HB algorithm that could describe multi-directional transport conditions to avoid later modifications. The present HB algorithm may be added to any profile response model that computes the net transport rate distribution, because the algorithm describing the constraint that the HB imposes on the transport rate does not depend on how this rate is calculated.

Theory and Numerical Implementation

The net transport rate is first calculated at all grid points across shore neglecting the presence of a possible HB, and this quantity represents the potential transport rate q_p. If the HB is or will become exposed during the calculation time-step, constraints must be placed on the transport rate so that the profile elevation remains fixed along profile segments where the HB is exposed

(it is assumed here that the HB is nonerodible). By employing the sand volume conservation equation, the calculated depth changes based on q_p will indicate where HB may restrict the transport and profile change. The sand volume conservation equation is written

$$\frac{\partial q}{\partial x} = \frac{\partial h}{\partial t} \tag{1}$$

where q is net cross-shore transport rate, x is the cross-shore coordinate pointing offshore, h is the profile elevation taken positive below the still-water level (swl), and t is the time (see Figure 6 for a definition sketch). In the discretized form of an explicit solution scheme, Equation 1 becomes

$$h_j^{i+1} = h_j^i + \frac{\Delta t}{\Delta x}(q_{j+1}^i - q_j^i) \tag{2}$$

where Δt is the time-step, Δx is the length step, i denotes the step number in time, and j denotes the grid location along the profile. In the following, the index i has been dropped if all quantities are at the same time-step. Equation 2 is most conveniently solved on a staggered grid where the elevations are taken in the middle of a calculation cell and the transport rate at the boundaries.

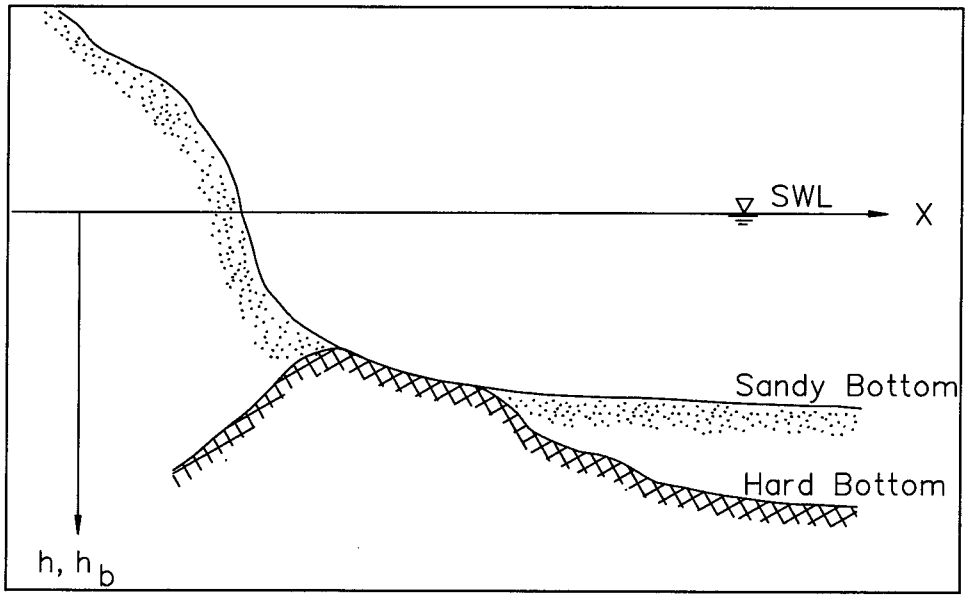

Figure 6. Definition sketch for algorithm to calculate the effect of hard bottoms on the profile evolution

The elevation of the HB, denoted as h_b, must be known at all grid points across shore. If the calculated potential profile elevation $h_{p,j} > h_{b,j}$ at time-step $i+1$ based on $q_{p,j+1}$ and $q_{p,j}$, then correction of the transport rate is needed because the calculated profile has moved below the HB. It is only if $\partial h/\partial t > 0$ that HB may constrain the transport rate. (The condition $\partial h/\partial t < 0$ implies accumulation, in which case the HB is assumed to have no effect, which is equivalent to

$\partial q/\partial x < 0$ according to Equation 1.) Thus, if $q_{p,j+1} < q_{p,j}$ the HB will have no effect and transport corrections are not needed unless updrift conditions influence the transport or elevation at this location. In the opposite case ($q_{p,j+1} > q_{p,j}$), the HB may restrict the transport if it is exposed or if there is not enough material in the cell above the HB elevation to satisfy the calculated potential depth change. A limited volume of sand ΔV_j available in cell j yields the following condition on the change in transport Δq_j (= q_{j+1} - q_j, where q denotes the correct transport rate that fulfills the HB constraints)

$$\Delta V_j = \Delta q_j \Delta t = (h_{b,j} - h_j)\Delta x \tag{3}$$

implying that it is only the volume of sand available between the profile elevation h_j and the HB elevation $h_{b,j}$ that is available for transport. If the HB is already exposed in a particular cell, $h_j = h_{b,j}$ and $\Delta q_j = 0$.

As seen from Equation 3, the HB restricts the change in the transport along the calculation grid. This means that the HB may only influence points that are downdrift (in the direction of transport) of the location where HB is exposed. Thus, an algorithm for correcting the transport rate must not only identify points where HB constrains the transport, but, because the conditions at neighboring grid points are coupled through Equation 3, restrictions imposed by updrift laying HB must also be checked. Corrections should be made in the direction of q, and HB can only influence segments along the profile where q has the same sign. Within each such segment the corrections should proceed from the updrift end to the point where the transport changes sign (or to the end of the grid, whichever is first encountered).

After computing q_p in the present algorithm, the number and locations of segments with different transport direction (onshore or offshore) are determined. The boundaries of such transport segments are given by $q_p = 0$, and consist of either cells at the end of the grid, divergence cells, or convergence cells (see Figure 7; also, compare the terminology minus and plus cells used by Hanson and Kraus (1985, 1987) for the two latter types of cells). A divergence cell has transport out of the cell at both boundaries, whereas a convergence cell experiences transport into the cell at the boundaries. Within each segment, a check is made to ascertain if the HB is exposed or will become exposed during a certain time-step by employing the criterion $h_{p,j} > h_{b,j}$, where $h_{p,j}$ is calculated based on q_p. If this is the case, the transport is corrected starting at the updrift end of the segment, which is a divergence point or the end of the grid, and stopping at a convergence point or the end of the grid. Across segments where the transport is directed offshore, the corrections proceed toward the offshore.

If the correction of the transport rate starts in a divergence cell, and the HB in this cell will become exposed during a certain time-step, it is not possible to uniquely determine how material is transported out of the cell (Hanson and Kraus 1985, 1987). The most straightforward assumption is that the material is transported at the left and right boundaries in proportion to the respective potential transport rates at the boundaries. In this case, the corrected transport rates may be written

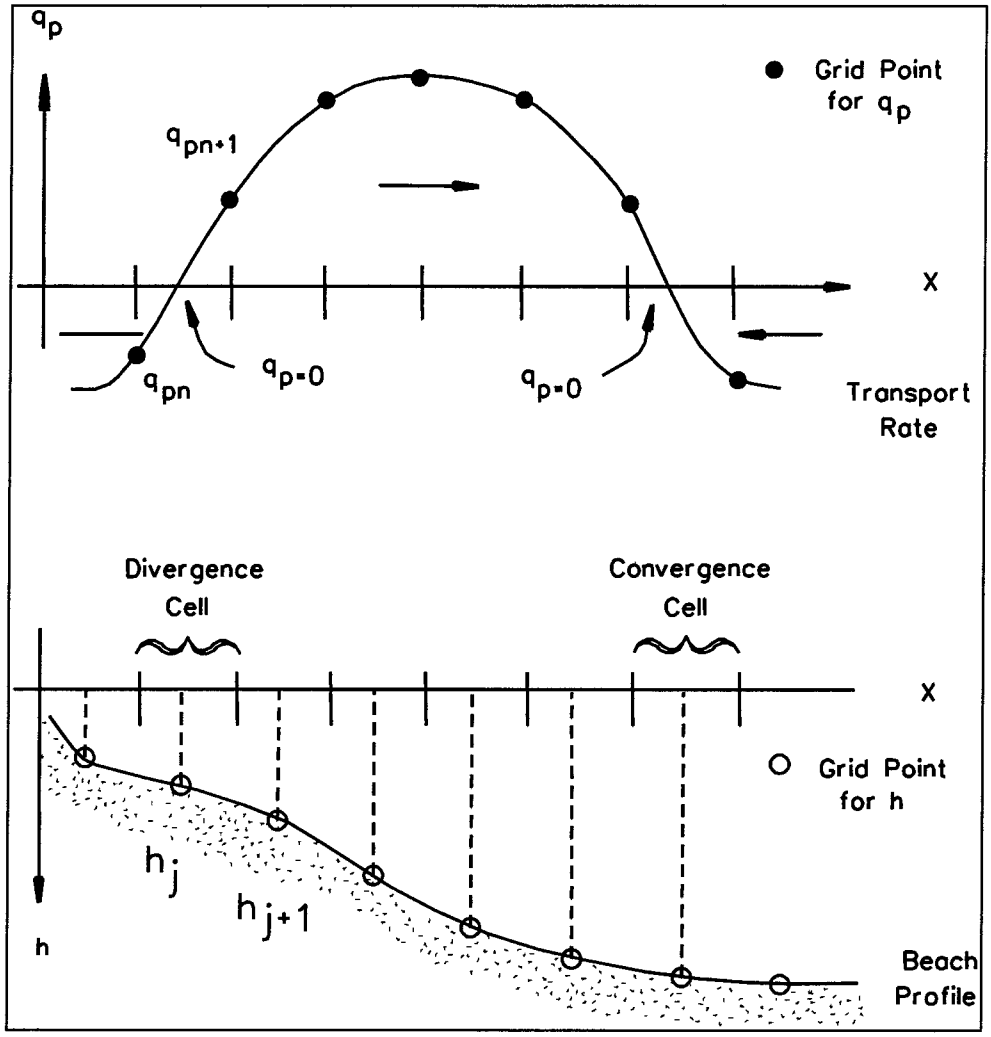

Figure 7. Schematic of convergence and divergence cells together with grid for calculating transport rate and profile change

$$q_j = \frac{q_{p,j}}{q_{p,j+1} - q_{p,j}} (h_{b,j} - h_j) \frac{\Delta x}{\Delta t}$$

$$q_{j+1} = \frac{q_{p,j+1}}{q_{p,j+1} - q_{p,j}} (h_{b,j} - h_j) \frac{\Delta x}{\Delta t} \qquad (4)$$

where j is the number of the divergence cell (note that $q_{p,j+1} > 0$ and $q_{p,j} < 0$ for a divergence cell, so the denominator can never be zero). Equation 4 may be manipulated to give expressions identical to those that Hanson and Kraus (1985, 1987) obtained for their corresponding "minus cells"

$$q_j = q_{p,j}\frac{h_{b,j} - h_j}{h_{p,j} - h_j}$$
$$q_{j+1} = q_{p,j+1}\frac{h_{b,j} - h_j}{h_{p,j} - h_j} \qquad (5)$$

where $h_{p,j}$ is the potential depth at time $i+1$ neglecting the HB.

An additional check must be made directly downdrift of areas where HB is exposed, because $\partial q/\partial x$ may change sign due to the HB corrections (see Figure 8). A transport gradient based on q_p may be negative, which means accumulation and no risk of HB exposure; however, after corrections are made, the presence of exposed HB may cause a positive gradient in q to appear downdrift of the HB area. The signs could be reversed if q_p has been reduced along the HB area in order to obtain q, whereas $q = q_p$ downdrift of the area. Additional HB exposure may occur that must be treated by the algorithm.

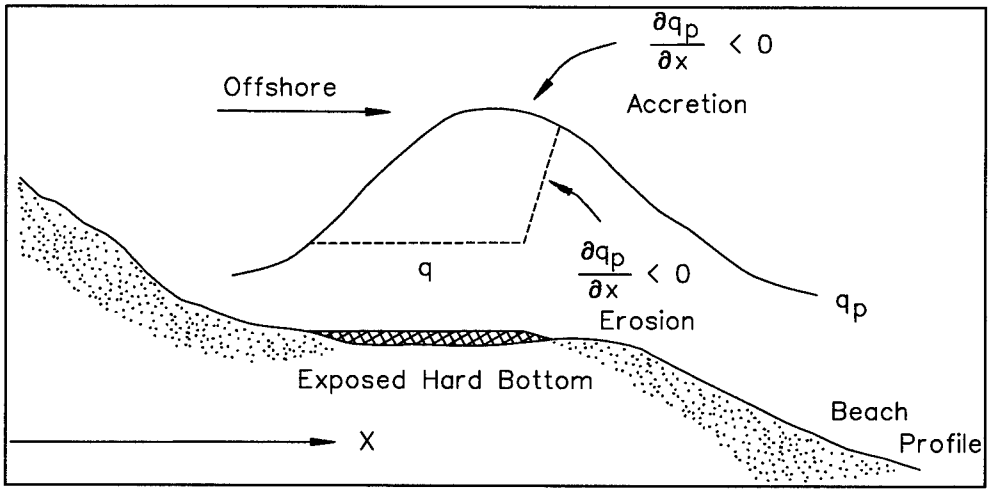

Figure 8. Schematic of the effect of transport corrections downdrift of an exposed hard bottom area

Downdrift of an exposed HB area, significant scour can appear if h_b increases at a steep gradient ($h_b > 0$ below swl, as before). In reality, for a fixed set of wave and water level conditions, it is expected that such scour would only continue until some equilibrium depth (Hoffmans and Pilarczyk 1995) is attained, after which there would be no further local erosion. However, the model might not properly describe this situation and could overestimate the scour, depending on the HB configuration. A simple means of limiting the scour downdrift of HB was introduced in the HB algorithm. It is assumed that the transport rate increases exponentially with distance downdrift of the HB to the potential value q_p, where the rate of increase is determined by an empirical parameter λ_{hb}, called the scour attenuation coefficient. The expression used in the algorithm is

$$q = q_p + (q_{hb} - q_p)e^{-\lambda_{hb}(x-x_{hb})} \qquad x \geq x_{hb} \tag{6}$$

where q_{hb} is the transport rate at x_{hb}. Equation 6 yields $q = q_{hb}$ if $x = x_{hb}$, and $q = q_p$ as $x \to \infty$. A larger value of λ_{hb} allows a more pronounced scour hole to develop than a smaller value. A value of $\lambda_{hb} = 1.0\ m^{-1}$ is presently implemented, but this value must be examined in the future based on experience with the model and validation with field and laboratory measurements.

Sample Calculations with the Hard-Bottom Algorithm

Sample calculations were performed for hypothetical transport rate distributions and profile and HB configurations to test and evaluate the properties of the basic HB algorithm. These calculations were made in a stand-alone program separate from SBEACH in order to more easily analyze the performance of the HB algorithm and to allow testing of situations that are more complex than those that are presently possible to simulate realistically with SBEACH. The results from selected sample calculations are presented below to illustrate how the HB algorithm operates.

In the calculations presented here, an equilibrium profile was selected as the initial profile that was identical to the profile employed by Kraus and Smith (1994) in SUPERTANK Test ST_10. The HB elevations were given at all points across shore, and HB was exposed along certain portions of the profile. A potential net cross-shore transport rate distribution was applied that was formed as a sum of Gaussian curves, each one with a specified standard deviation and mean, and with a maximum value that was +1 (offshore) or -1 (onshore). The sand conservation equation (Equation 1) was then employed together with the HB algorithm to compute the profile change resulting from the applied potential transport rate distribution. The duration of the calculation was selected so as to produce a reasonable amount of profile change. In the presented calculation results, the values of the input parameters are not of importance; focus is on the qualitative predictive behavior of the HB algorithm.

Figure 9 displays the calculation results for a potential transport rate distribution with one positive (offshore-directed transport) peak and with initially exposed HB between 15 and 25 m. The HB was made to slope downward at 1V:5H on both sides of the exposed HB. Figure 9a shows the calculated profile change, with erosion in the nearshore and deposition in the offshore where a bar-like feature is formed. The HB prevents lowering of the profile in areas where it has become exposed. The calculated profile exposes more HB than the initial profile because a scour hole formed downdrift of the initially exposed HB. The scour attenuation coefficient λ_{hb} was set to $1.0\ m^{-1}$ in the calculations to produce what were considered to be reasonable results; appropriate values of this parameter should be determined by comparison to measurements (see discussion, next section).

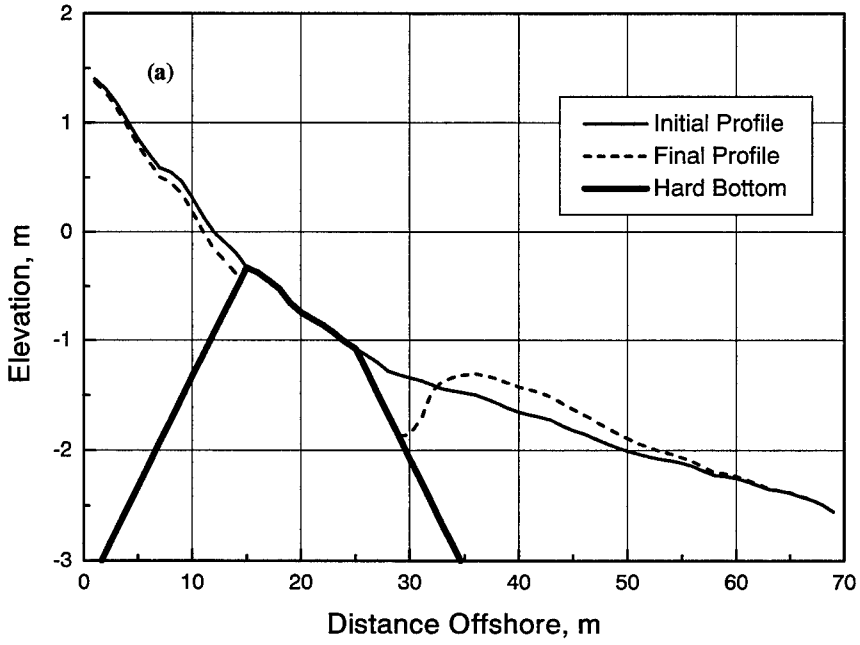

a. Profile change around hard bottom

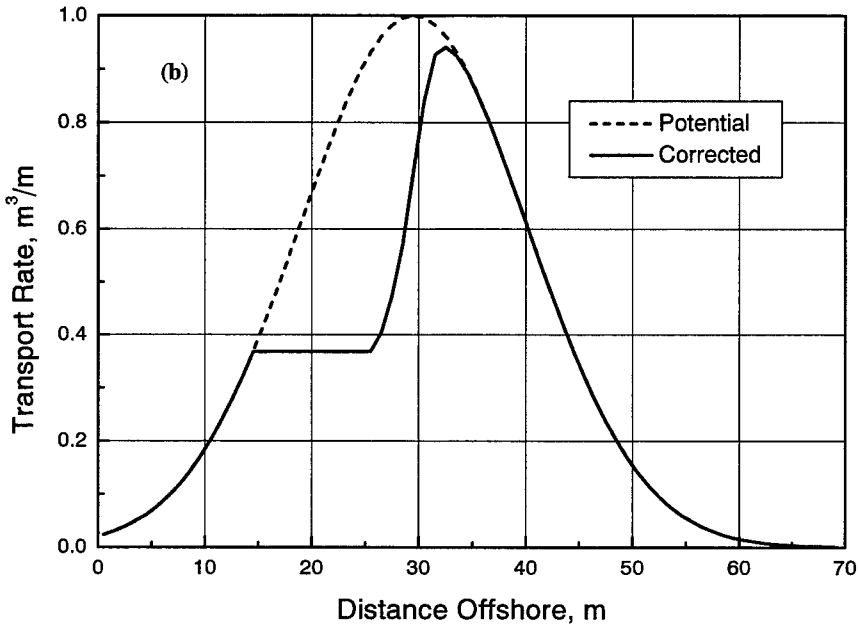

b. Potential and corrected transport rate

Figure 9. Sample calculation with one positive peak and initially exposed HB between 15 and 25 m

The potential transport rate q_p and the corrected transport rate q that fulfills the HB constraint are illustrated in Figure 9b. The Gaussian-shaped q_p yields erosion in the nearshore because $\partial q_p/\partial x > 0$; however, in the area where the HB is exposed, no material is available to sustain this erosion; the transport coming from the updrift side of the HB cannot increase, and the transported material simply passes along the exposed HB. Downdrift of the HB area, q increases to approach q_p because sand is available to maintain the potential transport. However, the growth in q is gradual, mainly because additional HB is becoming exposed, and the amount of sand available on top of the HB is limited.

Figure 10 shows the profile change and transport rate distributions, respectively, for a slightly more complicated situation. The q_p-distribution has one positive and one negative peak, implying that sand is eroded in the nearshore as well as in the offshore. The material is deposited in the middle section of the profile. Furthermore, there are two areas where the HB is exposed initially, namely along the sections running from 10 to 20 m and from 40 to 50 m.

The calculated profile change exhibits somewhat unrealistic deposition (Figure 10a; note the pronounced feature in the middle of the profile). The unrealistic deposition is the result of calculating for a single, fairly long time-step without feedback between the profile and the transport rate, in contrast to the shorter time-steps and continual feedback that occur in SBEACH. Additional HB is exposed during the calculation downdrift of both HB areas (downdrift refers to different directions for the two HB areas, because q has different directions in the areas). Also, updrift of the seawardmost HB area, local erosion leads to additional HB exposure as sand moves seaward over the HB.

The corrected transport rate that satisfies the HB constraints is displayed in Figure 10b, together with q_p. The exposed HB restricts the sand transport for both the positive and negative peak, and along these stretches of HB the sand is simply conveyed towards the deposition area located in the middle of the grid (determined by $\partial q/\partial x < 0$). In the HB algorithm, modifications to q_p are always made in the direction of transport. For example, in Figure 10b, the potential rate q_p only changes sign once, producing two segments within which q_p has the same direction. In the most onshore-located segment ($q_p > 0$), modification of q_p proceeds from the shoreward end of the grid to the cell where $q_p=0$ (convergence cell). For the seawardmost segment ($q_p < 0$), the modifications are made from the seaward end of the grid to the same convergence cell.

The empirical parameter λ_{hb}, which controls how far downdrift of exposed HB q_p is fully attained, influences the profile evolution mainly for configurations where the HB slope is large downdrift of an exposed section. To evaluate sensitivity of predictions to this parameter, sample calculations were performed for different values on λ_{hb} using the same test case as shown in Figure 9, but with an HB that sloped off at 1V:2H away from the initially exposed HB area. Figure 11 displays the effect of changing λ_{hb} on the profile evolution directly downdrift of the HB area and on the transport rate, respectively.

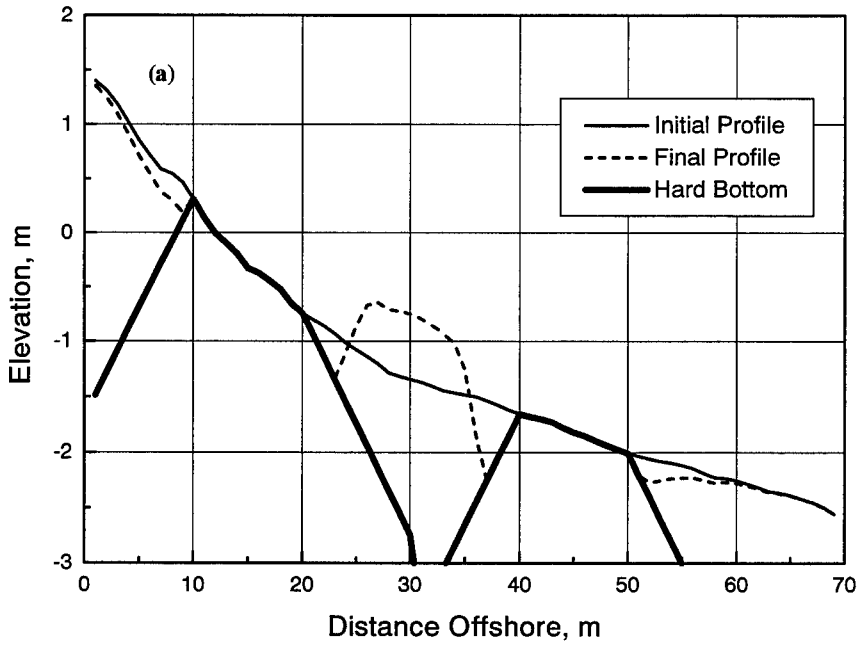

a. Profile change around hard bottom

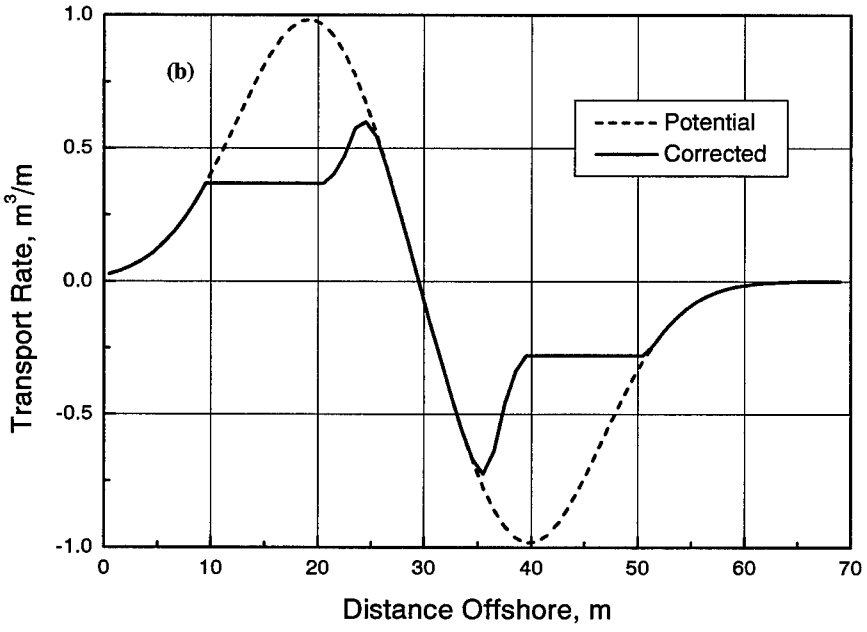

b. Potential and corrected transport rate

Figure 10. Sample calculation with one positive and one negative peak and initially exposed HB between 10 and 20 m and 40 and 50 m

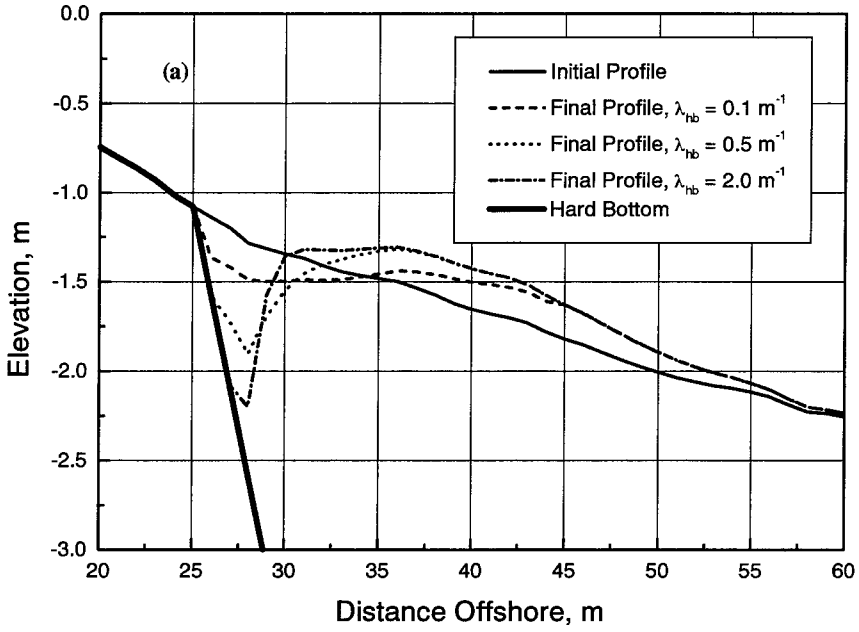

a. Effect on profile shape

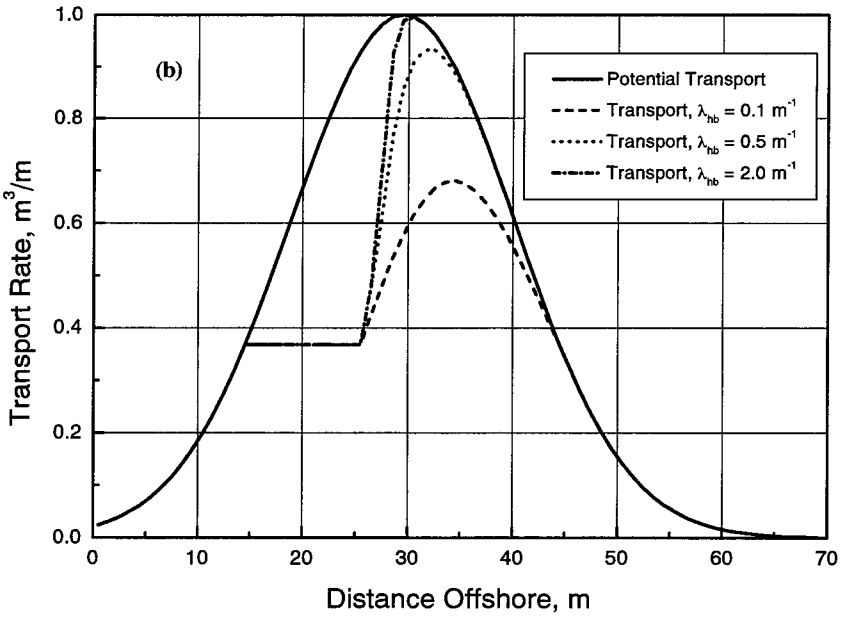

b. Effect on transport rate

Figure 11. Effect of changing the scour attenuation coefficient λ_{hb}

The effective range of λ_{hb} on the profile response is limited for the values selected (Figure 11a is an enlargement of the area at the downdrift end of the HB area). A value of $\lambda_{hb} = 2.0\ m^{-1}$ produces profile response that is similar to the case with no exponential transition towards q_p (or $\lambda_{hb} \rightarrow \infty$), implying development of a large scour hole. Smaller values on λ_{hb} still produce a clear scour hole, but with a shape and depth that appear more realistic than for larger values. The effect on q is shown in Figure 11b, where larger values of λ_{hb} yield a growth in q towards q_p at a steep gradient, which gives rise to the large gradient in q and the associated marked scour hole.

3 Comparisons to Physical Model Results

The physical and mathematical contexts of the HB algorithm were presented in the preceding chapter, together with a description of the numerical implementation within SBEACH. No field data were available with which to check the model predictions. However, data appropriate for testing SBEACH were found in prototype-scale physical model experiments performed in Germany and in smaller scale physical model experiments conducted in the United States. This chapter compares numerical simulations with measurements made in movable-bed physical models.

Data from the German Large Wave Tank

The sample calculations in the previous section showed that the HB algorithm developed in this study worked satisfactorily and produced qualitatively acceptable results. However, in order to quantitatively evaluate the algorithm and determine appropriate values of the scour attenuation coefficient λ_{hb} (Equation 6), data on profile evolution involving exposed HB must be employed. The most suitable data set reported in the literature for testing the HB calculation algorithm and SBEACH is that of Dette and Uliczka (1986, 1987). They performed experiments on beach profile change in a large wave tank (Groβe Wellen Kanal or GWK) in Germany, where large waves and realistic beach change can be generated without physical model scale effects. During one experimental case, a significant portion of the sloping cement bottom underlying the sand in the tank was exposed, restricting the supply of material. The sloping cement bottom was emplaced to reduce the amount of sand needed to form the beach. Exposure of the cement bottom in one fortuitous run provides measurements for evaluating the HB algorithm.

The GWK is 324 m long, 7 m deep, and 5 m wide (Dette and Uliczka 1986). In the case of interest, a dune without foreshore was emplaced in the tank with seaward slope of 1V:4H from an elevation of 2 m above the swl to the bottom of the tank located 5 m below swl. The sand had a median grain size of D_{50} = 0.33 mm, and the beach was subjected to monochromatic waves with height H = 1.5 m and a period T = 6.0 sec. These wave and sediment properties produced a markedly erosive condition, and the wave action rapidly removed material from the dune and deposited it in the offshore. The experiment was performed in bursts of as many as 80 waves to minimize seiching due to wave reflection, and

profile surveys were done between wave bursts. After an experimental duration of less than 200 waves, so much sand had been eroded from the dune that the sloping fixed cement bottom behind the dune was exposed, limiting further profile retreat in that area. This fixed bottom also had a slope of 1V:4H, as did the initial dune slope, and the result of exposure of the HB on profile evolution became similar to that expected on a sloping revetment.

To test the HB algorithm against data on profile evolution, the algorithm was implemented in SBEACH (Larson and Kraus 1989; Larson, Kraus, and Byrnes 1990; Rosati et al. 1993; Wise, Smith, and Larsen 1995) as discussed in Chapter 2. Initially, SBEACH was run with default values of all calibration coefficients as determined from previous use of the model to other large wave tank (LWT) data and to field data (Wise, Smith, and Larson 1996). The main calibration parameter is the coefficient K in the sand transport rate equation (Larson and Kraus 1989); a larger value of K implies a more rapid response of the profile to the incident waves. Two other coefficients are available to modify the calculated profile response, namely, the coefficient for the slope-dependent transport ϵ and the coefficient λ that describes the decay of the transport seaward of the break point. The coefficient λ depends upon the grain size and breaking wave height (Larson and Kraus 1989), and SBEACH has the option of specifying a constant multiplier C_λ in this relationship to account for site-specific conditions.

The use of the default value on K (= 1.75 10^{-6} m^4/N) produced a profile response that was somewhat too slow as compared to the GWK profile survey measurements, and K was increased to improve the agreement. A value of K = 2.5 10^{-6} m^4/N produced satisfactory agreement (at the moment, this is the largest value of K that can be specified in the SBEACH interface). The other coefficients were given the values ϵ = 0.001 m^2/sec and λ = 0.25 m^{-1}, which are somewhat smaller values than the original default values. The HB algorithm involves the scour attenuation coefficient λ_{hb}, and a value of 0.2 m^{-1} was selected mainly based on experience with the idealized simulations. Because the fixed bottom in the GWK case had a rather gentle slope for an HB "side," varying λ_{hb} did not markedly affect the calculation result; thus, the GWK data do not provide an adequate physical situation for determining an optimal value on λ_{hb}. It should be pointed out that the GWK data do provide a severe test for a profile response model because of the steep slope of the initial profile. Nairn and Riddell (1992), who performed simulations with a profile change model for a physical model case from Hughes and Fowler (1990) (discussed in the next section), which had a similar initial steep slope, did not start their calculations from the initial profile but substituted a profile surveyed at later times in the experiment. A more mildly sloping initial profile was probably used to avoid instabilities in the simulations.

Figure 12 displays the initial, calculated, and measured profiles together with the location of the HB (sloping fixed bottom) after 40, 370, 750, and 1,750 waves. The measured profile after 40 waves (4 min) displays a feature around the location x = 25 m that is not predicted by the model; this feature is most likely the result of initial collapse of the steep dune face as it was attacked by the waves. SBEACH can only schematically represent this type of profile change through avalanching algorithm. The profile retreat above SWL is fairly well predicted after 40 waves, although there is a small lag in the calculated

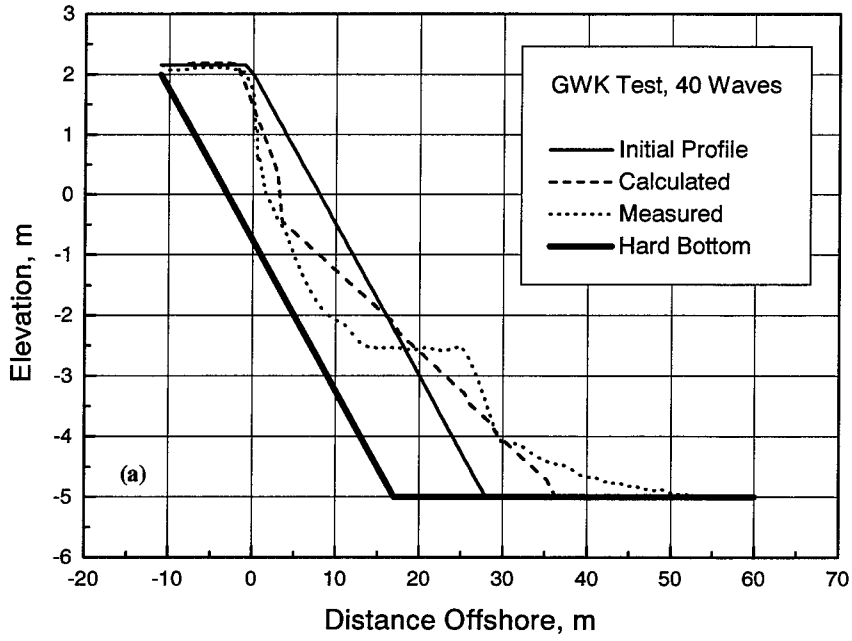

a. Profiles after 40 waves

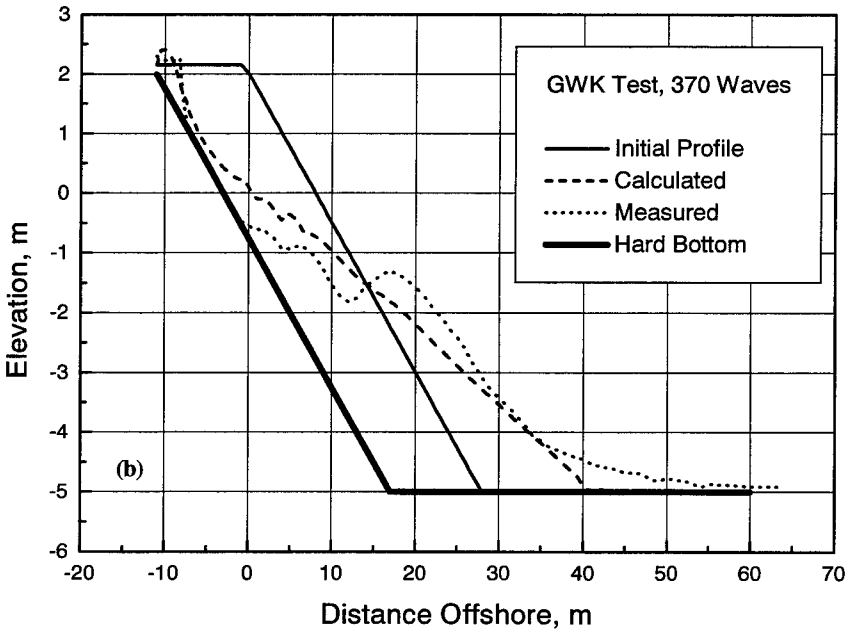

b. Profiles after 370 waves

Figure 12. Calculated and measured profiles for the case of Dette and Uliczka (1986) (Continued)

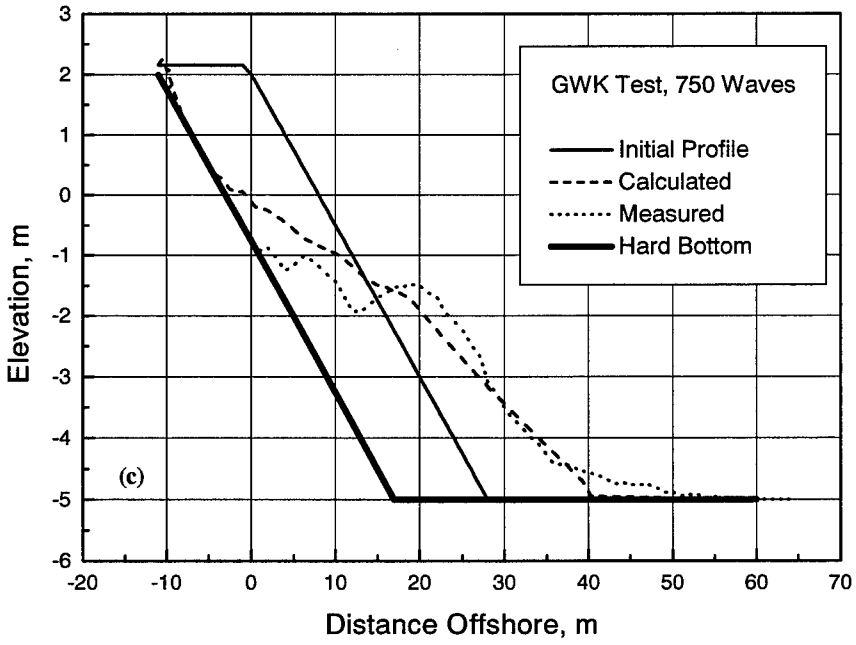

c. Profiles after 750 waves

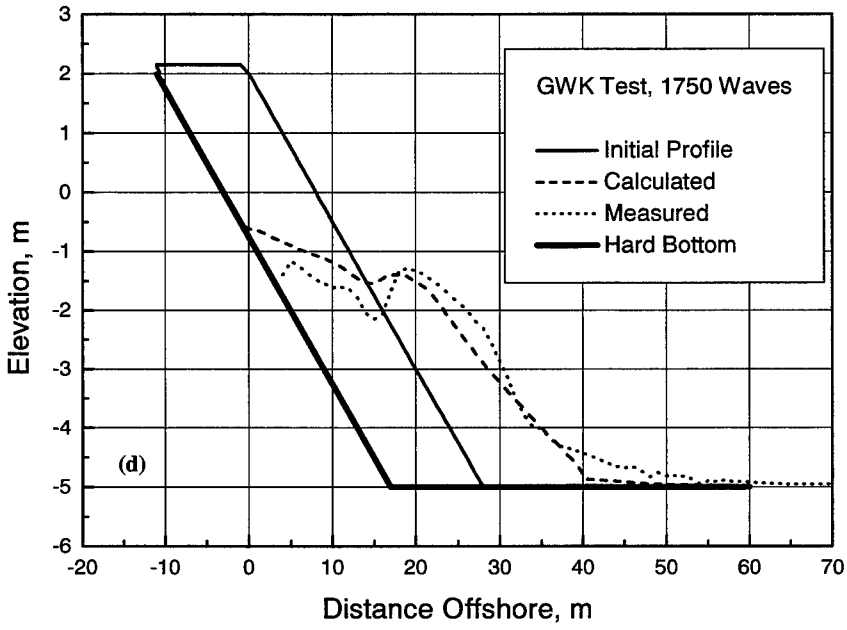

d. Profiles after 1,750 waves

Figure 12. (Concluded)

profile response. The lag is more evident in Figure 12b (profile after 370 waves or 37 min), where the measured profile shows that the erosion had then reached the fixed bottom; in the calculated profile, the fixed bottom is still covered with sand. The measured bar-like feature in the offshore does not appear in the calculated profile, which has a monotonically decreasing shape in the offshore. Overall, the steeply sloping profile prevents development of a bar in the calculations. The small hump of sand in Figure 12b at the top of the dune appearing in the calculations is produced by overtopping (Wise and Kraus 1993; Wise, Smith, and Larson 1996); the measurements seem to indicate the presence of a similar feature.

In Figures 12c and 12d, the calculated profiles have retreated enough to expose the fixed bottom. The calculations still produce less erosion than measured, but the difference is smaller than at earlier times. Also, after 1,750 waves (175 min; Figure 12d) a small feature developed in the proper location, although it is not as pronounced as in the physical model. The calculated profile in Figure 12d is close to the equilibrium shape; therefore, a longer simulation time will only cause marginally more erosion and bar buildup. The measured profile at the end of the experiment is also close to equilibrium, which may be shown by comparing the profiles after 1,650 and 1,750 waves (not included here).

The SBEACH simulations for the GWK data involving exposure of fixed bottom show that the HB algorithm can realistically simulate the constraint exerted by HB on profile evolution. The discrepancy in the initial time response between the model simulations and the measurements is mainly attributed to difficulties in accurately calculating the transport rate for the steep initial dune profile. A comparison between the final calculated and measured profile (close to equilibrium) supports the applicability of the HB algorithm for accurately predicting how an HB may limit the supply of material for transport.

Scale-Dependence of SBEACH Empirical Coefficients

Only one prototype-scale data set was available for evaluating the HB algorithm, as described above. Although the simulation results shown in the previous section displayed close agreement with the measurements, it was desirable to validate the algorithm for other conditions. Hughes and Fowler (1990) performed mid-scale physical model experiments on beach profile evolution under various combinations of sloping revetments and seawalls. This data set is suitable for further testing of the HB algorithm if the physical model scale for SBEACH is resolved. Also, because beach profile change in the physical model was studied for both monochromatic and random waves, the data set provides an excellent opportunity for testing the monochromatic and random version of SBEACH together with the HB algorithm.

SBEACH was developed using data from LWTs involving monochromatic waves (Larson and Kraus 1989) and then validated with field data (Larson, Kraus, and Byrnes 1990; Wise, Smith, and Larson 1996). Although the

governing equations in SBEACH are based on physical principles, some equations were heuristically derived and include empirical coefficients. The values of these coefficients were determined based on LWT data and field data, and some of the coefficients effectively act as calibration parameters (for example, K). SBEACH has not been previously applied to laboratory-scale data and, because some of the empirical coefficients are dimensional, it is not clear that the typical range of values found valid for the field is appropriate at a smaller scale. Thus, a simplified set of the governing equations in SBEACH was studied as described next to determine possible scale effects of the coefficients.

The wave transformation, net cross-shore transport rate, and beach change may be calculated, respectively, with the following equations

$$\frac{dF}{dx} = \frac{\kappa}{d}(F - F_{st}) \tag{7}$$

$$\frac{\partial q}{\partial x} = \frac{\partial h}{\partial t} \tag{8}$$

$$q = K(D - D_{eq}) \tag{9}$$

where F is the wave energy flux and F_{st} is the corresponding stable value, D is the wave energy dissipation per unit water volume (=$1/d\ dF/dx$), D_{eq} is the corresponding equilibrium value, d is the total water depth, and κ is an empirical coefficient. Equations 7-9 constitute a simplification of the governing equations in SBEACH; the physics contained in the model are still represented by the equations. For the shallow water, the wave energy flux is

$$F = \frac{1}{8}\rho g H^2 \sqrt{gd} \tag{10}$$

where ρ is the density of water, g is the acceleration of gravity, and H is the wave height. At stable conditions (no further breaking or wave height decay), the wave height is given by $H_{st} = \Gamma d$, where Γ is a nondimensional empirical coefficient, and H_{st} may be substituted in Equation 10 to obtain F_{st}.

To proceed in the scaling analysis, in Equations 7-9, length is normalized by using a representative wave height H_ℓ and time is normalized by using a representative wave period T_ℓ. The normalization leads to the nondimensional equations

$$\frac{dF'}{dx'} = \frac{\kappa}{d'}(F' - F'_{st}) \tag{11}$$

$$q' = \frac{1}{d'}\frac{dF'}{dx'} - D'_{eq} \tag{12}$$

$$\frac{1}{8}\frac{\rho g^{3/2} K T_\ell}{H_\ell^{3/2}}\frac{\partial q'}{\partial x'} = \frac{\partial h'}{\partial t'} \tag{13}$$

where a prime denotes a nondimensional quantity, and

$$D'_{eq} = \frac{D_{eq}}{\frac{1}{8}\rho g\sqrt{gH_\ell}} \tag{14}$$

Thus, if the following conditions hold,

$$\frac{1}{8}\frac{\rho g^{3/2} K T_\ell}{H_\ell^{3/2}} = \text{Constant} \tag{15}$$

$$\frac{D_{eq}}{\frac{1}{8}\rho g\sqrt{gH_\ell}} = \text{Constant} \tag{16}$$

the equations will predict an identical nondimensional profile evolution in time $h'(x',t')$, where $h' = h/H_\ell$, $x' = x/H_\ell$, and $t' = t/T_\ell$.

Assuming ρ and g to be constant, Equations 15 and 16 yield two scaling conditions, numbered as 1 and 2:

$$\left(\frac{KT_\ell}{H_\ell^{3/2}}\right)_1 = \left(\frac{KT_\ell}{H_\ell^{3/2}}\right)_2 \tag{17}$$

$$\left(\frac{D_{eq}}{\sqrt{H_\ell}}\right)_1 = \left(\frac{D_{eq}}{\sqrt{H_\ell}}\right)_2 \tag{18}$$

Kriebel, Kraus, and Larson (1991) showed, based on data, that D_{eq} is directly proportional to the sediment fall speed w, and Equation 18 may therefore be rewritten:

$$\left(\frac{w}{\sqrt{H_\ell}}\right)_1 = \left(\frac{w}{\sqrt{H_\ell}}\right)_2 \tag{19}$$

Retaining the g inside the square-root sign of the denominator in Equation 19 produces a nondimensional parameter discussed by Kraus, Larson, and Kriebel (1991) for distinguishing erosional and accretionary events on a beach. Furthermore, under the assumption that K is constant for Conditions 1 and 2, Equations 17 and 19 may be combined to yield to the condition that the nondimensional fall speed H_ℓ/wT_ℓ should be constant.

As expected, preliminary simulations with SBEACH for the mid-scale data using default values displayed model calculations that overpredicted the speed of erosion. Thus, the conclusion is that K (and some of the other dimensional coefficients) is influenced by scale and, before applying SBEACH to smaller scale laboratory experiments, some adjustment is needed. An adjustment is, perhaps, *a priori* evident because K is a dimensional empirical coefficient.

As an indication of the relationship between K at prototype and model scale, Equation 17 gives the following

$$\frac{K_p}{K_m} = \left(\frac{H_p}{H_m}\right)^{3/2} \frac{T_m}{T_p} \tag{20}$$

where the subscript p denotes prototype, and m denotes model conditions. The ratio H_p/H_m is given by the geometric scale ℓ; however, a scaling law has to be selected to obtain T_p/T_m, and thus K_p/K_m. The Froude modeling law (Hughes 1993) is often used in coastal engineering applications, which yields $T_p/T_m = \ell^{0.5}$. Under this assumption, Equation 20 gives $K_p/K_m = \ell$; that is, K scales in proportion to the geometric scale. Thus, before applying SBEACH to the smaller scale laboratory data, K should be divided by the scale ratio ℓ.

Mid-Scale Experiment Comparisons

One of the main objectives of Hughes and Fowler (1990) was to validate scaling laws for physical models involving cross-shore sediment transport and erosion near structures. In order to confirm the validity of the scaling laws used, Hughes and Fowler reproduced in a mid-scale physical model the Dette and Uliczka (1986) case discussed in the previous section. The sediment was scaled with the fall speed parameter H/wT, and other quantities were specified through Froude scaling.

The mid-scale experiments were done at a geometric scale of 1:7.5 (scale ratio $\ell = 7.5$ between prototype and model). Using the fall speed parameter to scale the grain size yielded $D_{50} = 0.13$ mm in the model. The same grain size and initial beach profile configuration (scale-copy of the Dette and Uliczka case; dune without foreshore sloping at 1:4, with fixed bottom having the same slope

under the sand) were used in all cases, with the exception that a seawall was placed around the still-water shoreline in some tests. The duration of the tests was typically 1,850 waves during which several profile surveys were conducted. The basic wave- and water-level conditions were $H = 0.2$ m, $T = 2.2$ sec, and a water depth $d = 0.67$ m. In the random wave tests, either the root-mean-square (rms) or the significant wave height was set equal to 0.2 m to determine the statistical wave height that gave the profile evolution closest to that produced by monochromatic waves. Table 1 summarizes the Hughes and Fowler tests that will be used here (case numbering follows that of Hughes and Fowler) to evaluate SBEACH and the HB algorithm.

SBEACH was applied to simulate profile evolution in the five tests summarized in Table 1. The coefficient values obtained from the GWK case were scaled and used without further modifications to validate SBEACH with the HB algorithm. Thus, the coefficient values selected were $K = 0.33\ 10^{-6}$ m^4/N, $\epsilon = 0.0001$ m^2/s, $C_\lambda = 1.88$ m^{-1}, and $\lambda_{hb} = 1.5$ m^{-1}. The two empirical decay coefficients C_λ and λ_{hb} scale as $1/\ell$, implying that the values are larger in the model than in the prototype.

Table 1
Tests from Hughes and Fowler (1990) Employed in the Present Study

T03	Monochromatic waves, sloping revetment
T08	Random waves ($H_{rms} = H_{mono}$), sloping revetment
T09	Random waves ($H_{1/3} = H_{mono}$), sloping revetment
T10	Monochromatic waves, sloping revetment and seawall
T11	Random waves ($H_{1/3} = H_{mono}$), sloping revetment and seawall

Note: H_{rms}: rms wave height, $H_{1/3}$: significant wave height, H_{mono}: monochromatic wave height.

In the following, the simulation results are briefly discussed for each test. The final measured profile and one intermediate profile in the experiments are compared. The final profile was taken after 1,850 waves had run (except in T08, where the final profile is after 1,650 waves), whereas the intermediate profile shown is that developed after 370 waves.

Test T03. This test aimed at reproducing the previously described GWK case. Monochromatic waves were allowed to attack the dune without a foreshore, and a sloping revetment was placed under the sand. Figure 13 compares SBEACH calculations and the mid-scale physical model results. The profile retreat predicted by SBEACH is somewhat greater than the measurements after 370 waves (note the distinct measured scarp in Figure 13a), and the calculations do not show the pronounced offshore bar obtained in the physical model at this elapsed time. Also, the revetment is not yet exposed. However, after 1,850 waves, the entire revetment above swl is uncovered, which is well predicted by SBEACH; also, the model predicts a bar at a location along the profile and with similar dimensions as those measured.

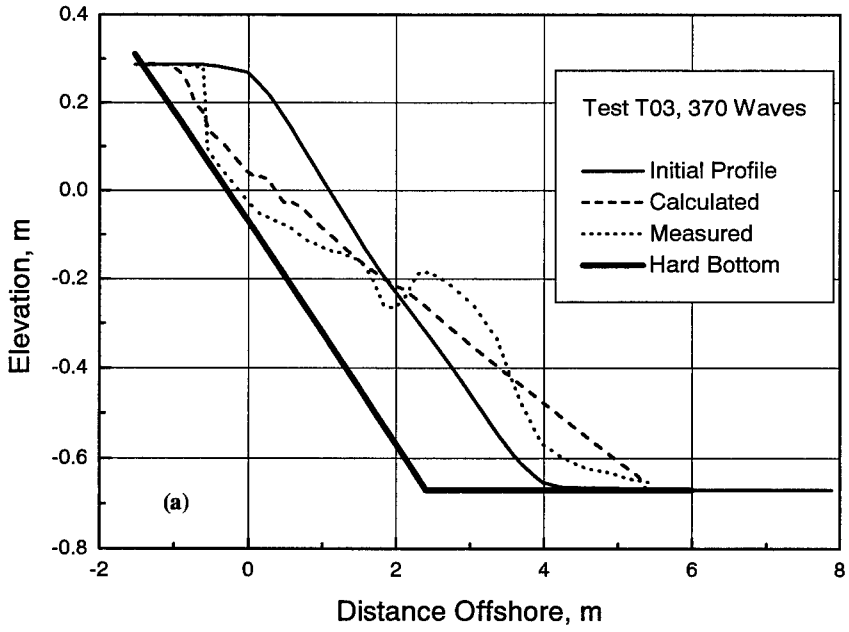

a. Profiles after 370 waves

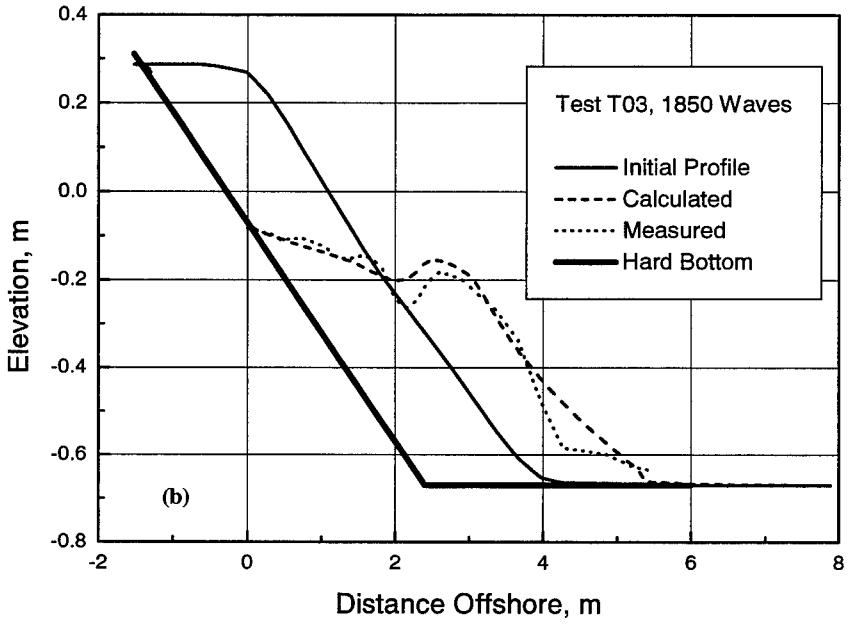

b. Profiles after 1,850 waves

Figure 13. Calculated and measured profile waves for Test T03 of Hughes and Fowler (1990)

Test T08. The experimental arrangement was the same as in T03, but random waves were employed with the rms wave height equal to the monochromatic wave height (implying an equal amount of wave energy for the two wave conditions). Agreement between calculations and the physical model seems to be better than for Test T08, especially after 370 waves (Figure 14a), although the calculated profiles are smoother than the measured. The slight bar feature occurring in the measured profile after 1,650 waves (Figure 14b) is not described by the numerical model. Comparison with Figures 13a and 13b shows the difference in profile change calculated with random waves and with monochromatic waves. The bar feature in Figure 13b is absent in Figure 14b because of the smoothing effect of random waves.

Test T09. This test was also identical to Test T03, except that the significant height of the random waves was set equal to the monochromatic wave height, implying that the random waves in total had less total energy than the monochromatic waves. Figure 15 illustrates the calculated profiles and the corresponding measurements. As in the calculations for Test T03, SBEACH predicts a profile retreat that is somewhat more rapid than the measurements. The overall agreement and the calculated exposure of the revetment seem satisfactory.

Test T10. A seawall was placed around the still-water shoreline and covered with sand, with the sloping revetment still in place. Monochromatic waves were employed, causing the profile to retreat rapidly and uncover the seawall. Figure 16 shows the calculated and measured profiles after 370 and 1,850 waves. The seawall in the physical model is completely exposed after 370 waves, whereas the sloping revetment is still covered with sand. This development is predicted well by the numerical model; as before, the bar feature in the offshore does not appear in the model calculations after 370 waves. However, after 1,850 waves, SBEACH produces a clear bar, although the crest is located somewhat inshore of the measured bar. Also, the marked observed trough in Figure 11 is absent in the numerical model calculations.

Test T11. This test was identical to Test T10 with the exception that random waves were used, where the significant wave height was set equal to the monochromatic wave height in T10. Calculations and measurements (Figure 17) agree somewhat better than for the monochromatic case. A distinct bar was not formed because of the smoothing produced by the random waves.

In summary, predictions of SBEACH produced satisfactory agreement with the measurements made in a mid-scale physical model. No special calibration was performed for the tests, with the empirical coefficient values determined for the GWK physical model comparison employed directly after appropriate scaling. SBEACH proved capable of not only giving realistic simulation results for the smaller scale experiments, but also for both monochromatic and random waves in various combinations with the shore-protection structures of sloping revetments and a seawall.

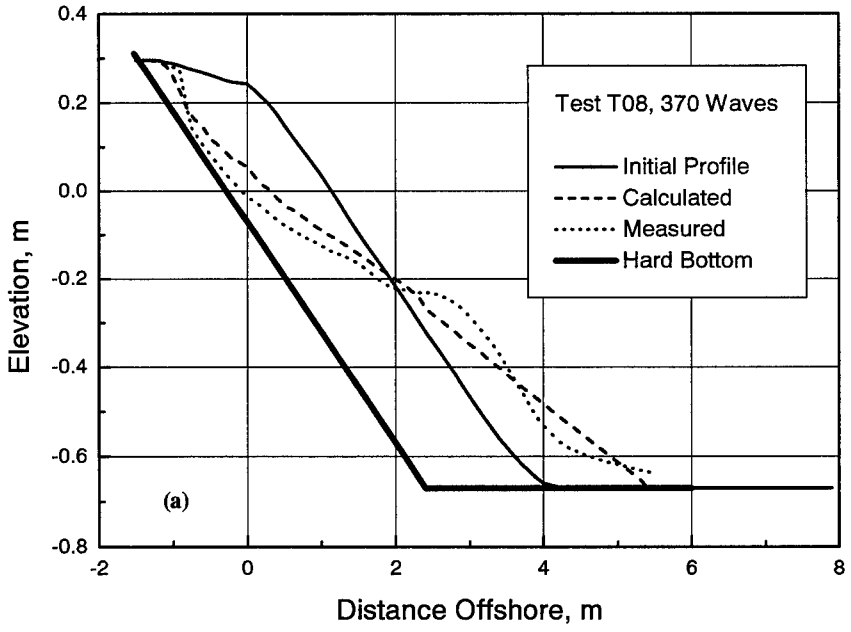

a. Profiles after 370 waves

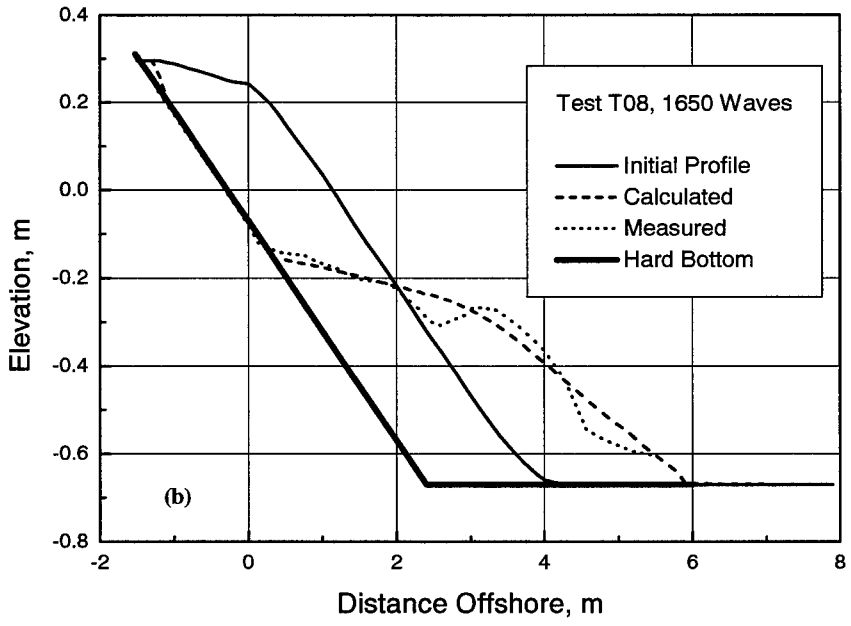

b. Profiles after 1,650 waves

Figure 14. Calculated and measured profiles for Test T08 of Hughes and Fowler (1990)

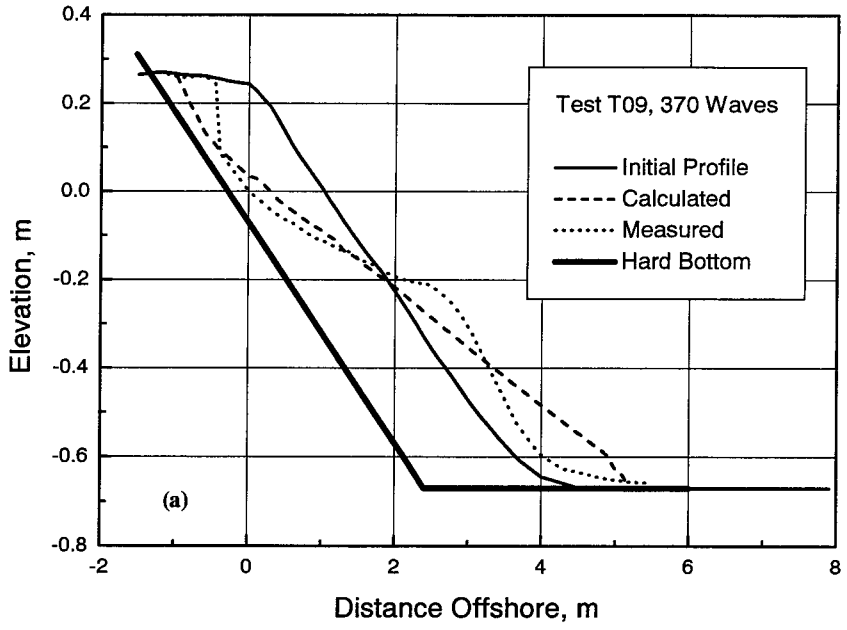

a. Profiles after 370 waves

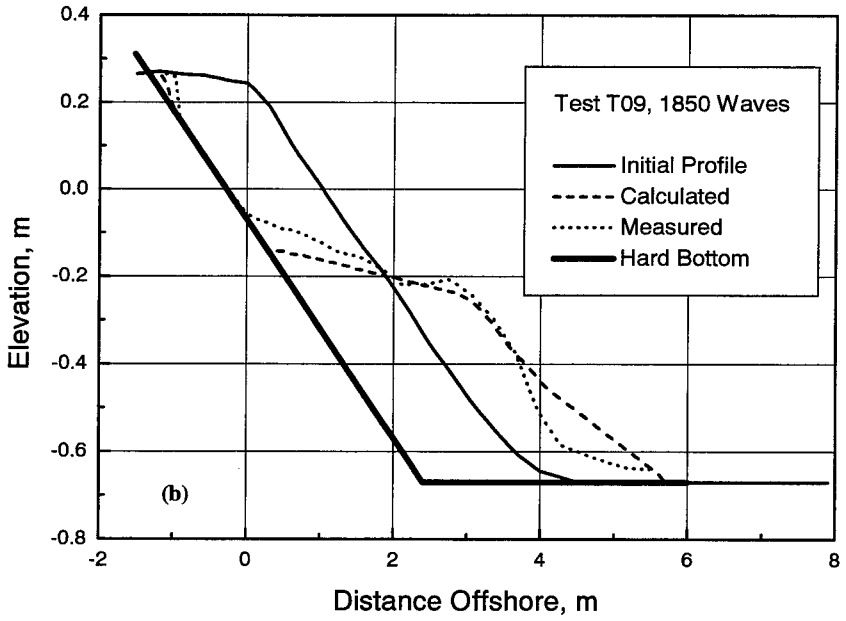

b. Profiles after 1,850 waves

Figure 15. Calculated and measured profiles for Test T09 of Hughes and Fowler (1990)

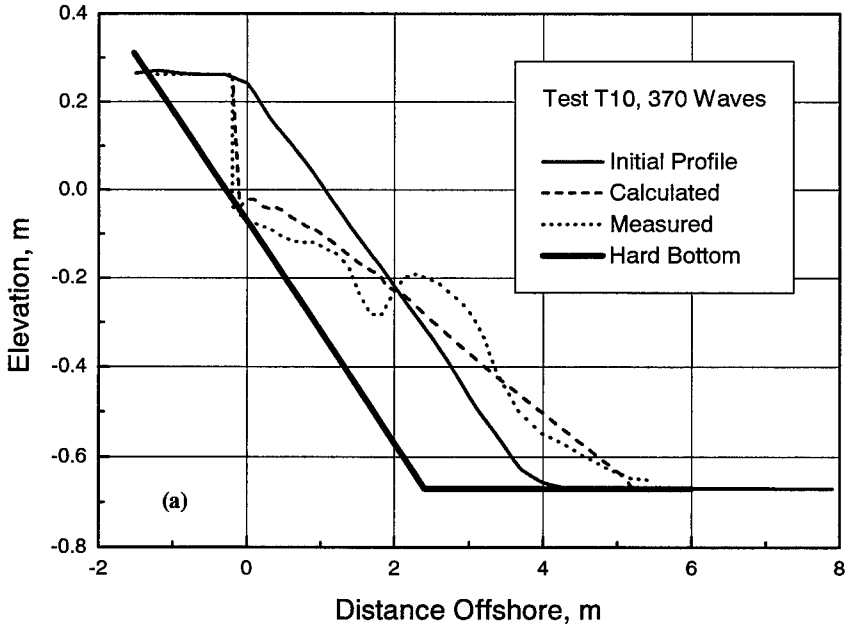

a. Profiles after 370 waves

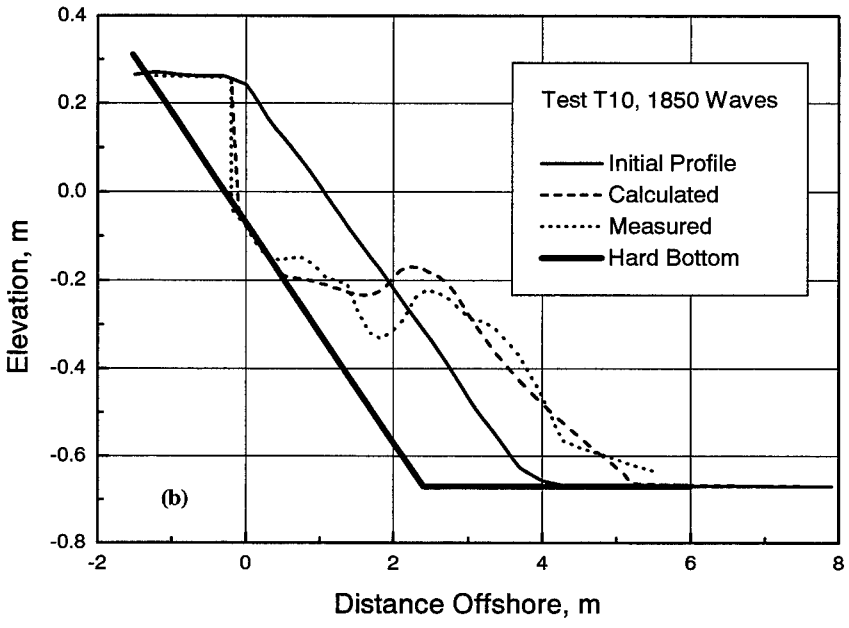

b. Profiles after 1,850 waves

Figure 16. Calculated and measured profiles for Test T10 of Hughes and Fowler (1990)

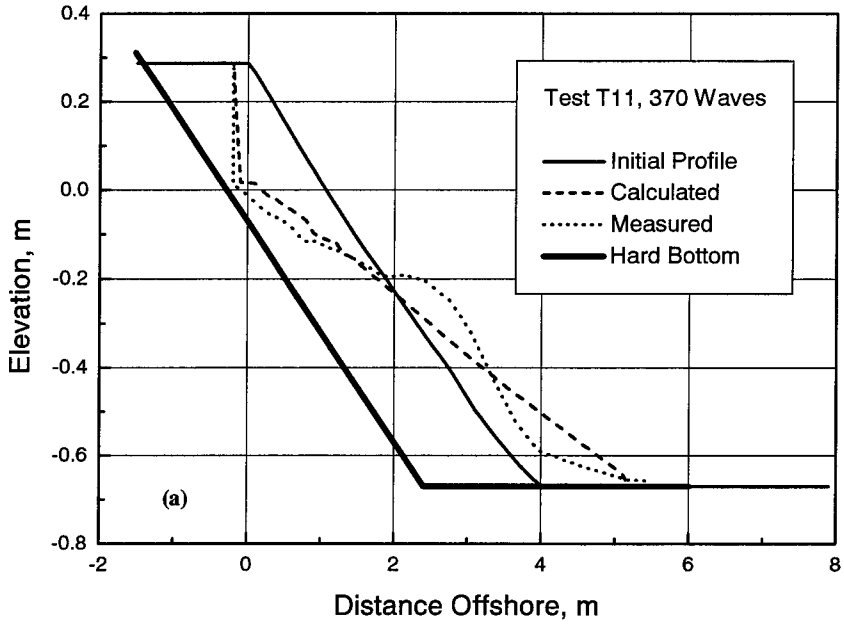

a. Profiles after 370 waves

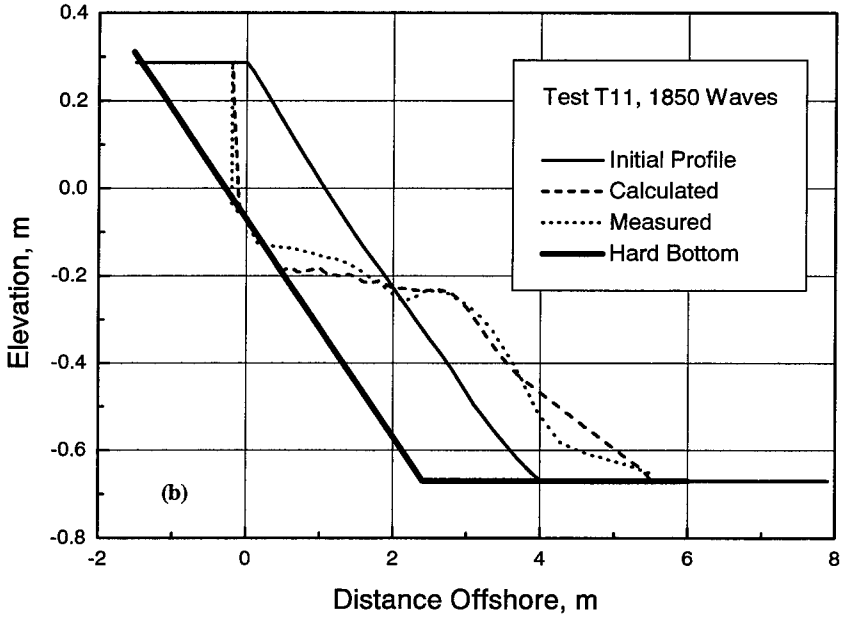

b. Profiles after 1,850 waves

Figure 17. Calculated and measured profiles for Test T11 of Hughes and Fowler (1990)

4 Concluding Discussion

In the present study, the SBEACH model was enhanced to account for a nonerodible (hard) bottom in the calculation domain. Arbitrary numbers and locations of HB can be specified.

Quantitative data were available for testing the HB algorithm. The HB implementation was evaluated in sensitivity tests for qualitative reasonability of results and was found to perform well. Quantitative tests through comparisons with a single available case of HB exposure in a large wave tank and with several tests performed with a mid-scale physical model were also successful. Comparisons with the mid-scale tests also validated the monochromatic and random-wave transport calculations. For comparison with the mid-scale tests, a scaling criterion was derived; success in reproducing the physical model results with SBEACH is an indirect confirmation that the basic physical principles acting to produce storm-induced beach erosion are represented in the numerical model.

Field data and physical model experiments are required to further validate and check the model, as well as to better understand the underlying physical processes. One task should be to understand the extent of scour at the margins of HBs. In reconnaissance of HB areas, it is important to know the subsurface configuration of the HB as, for example, whether it has near-vertical sides or slopes gently.

SBEACH is considered applicable to calculate storm-induced beach erosion on beaches containing HB areas in the nearshore. In this capacity, the model is expected to be an aid in design of beach fills and in guiding field-data collection as well as laboratory tests aimed at investigating the physical processes.

References

Dette, H. H., and Uliczka, K. (1986). "Velocity and sediment concentration fields across surf zones." *Proceedings of the 20th Coastal Engineering Conference*. American Society of Civil Engineers, 1,062-76.

_____. (1987). "Prototype investigations on time-dependent dune recession and beach erosion." *Proceedings of Coastal Sediments '87*. American Society of Civil Engineers, 1430-44.

Hansen, M., and Byrnes, M. R. (1991). "Development of optimal beach fill design cross-section." *Proceedings Coastal Sediments '91*. American Society of Civil Engineers, 2067-80.

Hanson, H., and Kraus, N. C. (1985). "Seawall constraint in shoreline numerical model," *Journal of Waterway, Port, Coastal, and Ocean Engineering* 111(6), 1,079-83.

_____. "Seawall boundary condition in numerical models of shoreline evolution," Technical Report CERC-87-9, U.S. Army Engineer Waterways Experiment Station, Vicksburg, MS.

Hoffmans, G. J. C. M., and Pilarczyk, K. W. (1995). "Local scour downstream of hydraulic structures," *Journal of Hydraulic Engineering* 121(4), 326-40.

Hughes, S. A. (1993). "Physical models and laboratory techniques in coastal engineering." *Advanced Series on Ocean Engineering*, Vol 7. World Scientific, Singapore.

Hughes, S. A., and Fowler, J. E. (1990). "Mid-scale physical model validation for scour at coastal structures," Technical Report CERC-90-8, U.S. Army Engineer Waterways Experiment Station, Vicksburg, MS.

Kraus, N.C., and Smith, J. M. (1994). "SUPERTANK laboratory data collection project; Volume I: Main text," Technical Report CERC-94-3, U.S. Army Engineer Waterways Experiment Station, Vicksburg, MS.

Kraus, N. C., and Wise, R. A. (1993). "Simulation of January 4, 1992 storm erosion at Ocean City, Maryland," *Shore and Beach* 61(1), 34-41.

Kraus, N. C., Larson, M., and Kriebel, D. L. (1991). "Evaluation of Beach Erosion and Accretion Predictors." *Proceedings of Coastal Sediments '91*. American Society of Civil Engineers, 572-87.

Kraus, N. C., Smith, J. M., and Sollitt, C. K. (1992). "SUPERTANK laboratory data collection project." *Proceedings of 23rd Coastal Engineering Conference*. American Society of Civil Engineers, 2191-2204.

Kriebel, D. L., Kraus, N. C., and Larson, M. (1991). "Engineering methods for predicting beach profile response." *Proceedings of Coastal Sediments '91*. American Society of Civil Engineers, 557-71.

Larson, M., and Kraus, N. C. (1989). "SBEACH: Numerical model for simulating storm-induced beach change; Report 1: Empirical foundation and model development," Technical Report CERC-89-9, U.S. Army Engineer Waterways Experiment Station, Vicksburg, MS.

_____. (1991). "Mathematical modeling of the fate of beach fill," *Artificial Beach Nourishments*, Special Issue of *Coastal Engineering*, H. D. Niemayer, J. van Overeem, and J. van de Graaff, ed., Vol 16, 83-114.

Larson, M., Kraus, N. C., and Byrnes, M. (1990). "SBEACH: Numerical model for simulating storm-induced beach change; Report 2: Numerical formulation and model tests," Technical Report CERC-89-9, U.S. Army Engineer Waterways Experiment Station, Vicksburg, MS.

Nairn, R. B., and Riddell, K. J. (1992). "Numerical beach profile modelling for beachfill projects." *Proceedings of Coastal Practice '92*. American Society of Civil Engineers, 12-28.

Nairn, R. B., and Southgate, H. N. (1993). "Deterministic profile modelling of nearshore processes; Part 2, Sediment transport and beach profile development." *Coastal Engineering* 19, 57-96.

Rosati, J. D., Wise, R. A., Kraus, N. C., and Larson, M. (1993). "SBEACH: Numerical model for simulating storm-induced beach change; Report 3, User's Manual," Instruction Report CERC-93-2, U.S. Army Engineer Waterways Experiment Station, Vicksburg, MS.

Smith, J. M., and Kraus, N. C. (editors). (1995). "SUPERTANK Laboratory Data Collection Project; Volume II: Appendices A-J," Technical Report CERC-94-3, U.S. Army Engineer Waterways Experiment Station, Vicksburg, MS.

Wise, R. A., and Kraus, N. C. (1993). "Simulation of beach fill response to multiple storms, Ocean City, Maryland," *Beach Nourishment Engineering and Management Considerations*. D. K. Stauble, and N.C. Kraus, volume eds. *Proceedings Coastal Zone '93*, American Society of Civil Engineers, 133-47.

Wise, R. A., Smith, S. J., and Larson, M. (1996). "SBEACH: Numerical model for simulating storm-induced beach change; Report 4, Cross-shore transport under random waves and model validation with SUPERTANK and field data," Technical Report CERC-89-9, U.S. Army Engineer Waterways Experiment Station, Vicksburg, MS.

Appendix A
Notation

d	Total water depth
D	Wave energy dissipation per unit water volume
D_{50}	Median grain size
D_{eq}	Equilibrium value
F	Wave energy flux
F_{st}	Wave energy stable value
g	Acceleration of gravity
h	Profile elevation taken positive below the still-water level
h_b	Elevation of the hard bottom
H	Wave height
$H_{1/3}$	Significant wave height
H_{mono}	Monochromatic wave height
H_{rms}	rms wave height
H/wT	Fall speed parameter
i	Step number in time
j	Grid location along the profile number of the divergence cell
k	Main calibration parameter
m (subscript)	Model conditions
p (subscript)	Prototype
q	Net cross-shore transport rate

q_{hb}	Transport rate at x_{hb}
q_p	Potential value
t	Time
T	Wave period
w	Sediment fall speed
x	Cross-shore coordinate pointing offshore
Γ	Nondimensional empirical coefficient
Δqj	Change in transport
Δt	Time-step
Δv_j	Limited volume of sand available in cell j
Δx	Length step
ε	Slope-dependent transport
κ	Empirical coefficient
λ	Coefficient that describes the decay of the transport seaward of the break point
λ_{hb}	Empirical parameter Scour attenuation coefficient
C_λ	Constant multiplier
ρ	Density of water
ℓ	Geometric scale
H_ℓ	Representation wave height
T_ℓ	Representative wave period

REPORT DOCUMENTATION PAGE

Form Approved
OMB No. 0704-0188

1. AGENCY USE ONLY *(Leave blank)*	2. REPORT DATE	3. REPORT TYPE AND DATES COVERED
	August 1998	Report 5 of a series

4. TITLE AND SUBTITLE
SBEACH: Numerical Model for Simulating Storm-Induced Beach Change; Report 5, Representation of Nonerodible (Hard) Bottoms

5.FUNDING NUMBERS

6. AUTHOR(S)
Magnus Larson, Nicholas C. Kraus

7. PERFORMING ORGANIZATION NAME(S) AND ADDRESS(ES)
University of Lund
Box 118, Lund, Sweden S-221 00
U.S. Army Engineer Waterways Experiment Station
3909 Halls Ferry Road, Vicksburg, MS 39180-6199

8. PERFORMING ORGANIZATION REPORT NUMBER
Technical Report CERC-89-9

9. SPONSORING/MONITORING AGENCY NAME(S) AND ADDRESS(ES)
U.S. Army Corps of Engineers
Washington, DC 20314-1000

10. SPONSORING/MONITORING AGENCY REPORT NUMBER

11. SUPPLEMENTARY NOTES
Available from National Technical Information Service, 5285 Port Royal Road, Springfield, VA 22161.

12a. DISTRIBUTION/AVAILABILITY STATEMENT
Approved for public release; distribution is unlimited.

12b. DISTRIBUTION CODE

13. ABSTRACT ***(Maximum 200 words)***

The SBEACH (Storm-induced BEAch CHange) numerical simulation model was developed at the U.S. Army Engineer Waterways Experiment Station to calculate beach and dune erosion under storm water levels and wave action. The work documented in this report was performed to allow SBEACH to account for nonerodible (hard) bottoms in computing dune and beach erosion. Sensitivity tests were used to evaluate the results of incorporating the HB factor into SBEACH. For qualitative reasonability of results, addition of the HB factor was found to perform well. Quantitative tests comparing a single available case of HB exposure in a large wave tank with several tests performed with a mid-scale physical model were also successful. Comparisons with the mid-scale tests also validated the monochromatic and random-wave transport calculations. For comparison with the mid-scale tests, a scaling criterion was derived; success in reproducing the physical model results with SBEACH is an indirect confirmation that the basic physical principles acting to produce storm-induced beach erosion are represented in the numerical model.

14. SUBJECT TERMS
Beach erosion
Dune erosion
Hard bottoms
Nonerodible bottoms
SBEACH

15. NUMBER OF PAGES
44

16. PRICE CODE

17. SECURITY CLASSIFICATION OF REPORT	18. SECURITY CLASSIFICATION OF THIS PAGE	19. SECURITY CLASSIFICATION OF ABSTRACT	20. LIMITATION OF ABSTRACT
UNCLASSIFIED	UNCLASSIFIED		